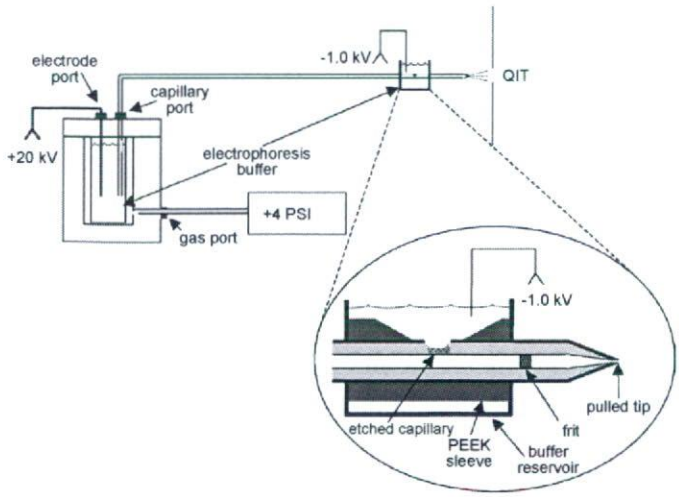

Fig. 1. Diagram of sheathless CE interfaced to quadrupole ion trap MS. Inlet of CE is pressurized for separation using the reservoir shown. Inset shows the etched porous junction. Reprinted from [56] with permission.

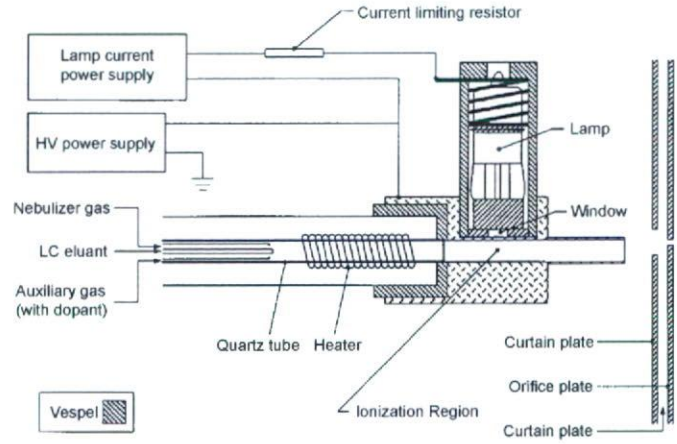

Fig. 2. Schematic of the APPI ion source, including the heated nebulizer probe, photoionization lamp, and lamp mounting bracket. Reprinted from [66] with permission. Copyright 2000 American Chemical Society.

utility was demonstrated by the detection of abnormal levels of amino acids in the blood of newborns afflicted with metabolic disorders.

Based on the principle of the electrospray process, i.e., protonation or deprotonation of solutes or formation of charged adducts, ESI is particularly suited for the analysis of polar compounds [60], but is rather inefficient for nonpolar ones. Moreover, it suffers from low tolerance of salts and susceptibility to matrix effects; thus, good resolution of sample components is important for limiting competing ionizations. With ESI for MS interfacing, the range of CE buffers is restricted to volatile types, which often do not provide the same separation performance as standard buffers for CE with UV detection, such as phosphate and borate. In addition, their concentrations must be kept low so as not to impair ion production, and this generally results in lower efficiencies [61]. By comparison, APCI has been demonstrated to be more tolerant of salts and other nonvolatiles [62,63]. Because ionization conditions are "harder" than those in ESI, it is more suitable for less polar compounds [64]. However, poor sensitivity has deterred its widespread acceptance. It is also not preferred for qualitative assays, such as metabolite identification, because it may produce in-source fragmentation of thermally unstable compounds [65]. APPI [66], a new soft ionization mode, has been shown to be relatively nondiscriminate of nonpolar compounds and reasonably tolerant of matrix additives [67]. The APPI interface (Fig. 2) uses a photoionization lamp and a dopant (a photoionizable molecule, e.g., acetone or toluene) to form dopant radical cations producing protonated eluent molecules, followed by a proton-transfer reaction with the analyte [65]. It has been rapidly adopted in LC–MS [65–69], but few papers regarding its use in CE–MS have been published so far. Nonvolatile buffers [61,70], and even sodium dodecyl sulfate (SDS) [71], the most common micelle used in MEKC, were reported not to affect its ionization efficiency. Thus, with its ability to ionize nonpolar compounds, APPI may be a more widely applicable ionization method for CE–MS. It must be noted, though, that there is an apparent trend toward a "single" ionization source containing combinations of ESI and APCI or ESI and APPI [72].

Almost all types of mass analyzers have been coupled to CE. Because of their relatively low cost, single quadrupoles (Qs) remain popular [32,51,54,57,73–79], though, mainly as mass-selective detectors. Ion traps (ITs) are employed more extensively [21,29,38,40,41,49,50,52,80–89], enabling tandem MS to be performed [21,40,85,86,88] without the need for multiple analyzers. However, the typically narrow peaks resulting from CE separations, in addition to sample complexity, have fueled interest in higher-performance instruments, which are capable of very fast scan speed necessary to adequately describe very sharp peaks, high mass range for expanded coverage, high mass accuracy, high resolution to be able to resolve closely migrating components with similar nominal masses, and/or multi-stage MS capabilities for unequivocal metabolite identification. Thus, triple quadrupoles [22,42,90–94], TOF [76,95–97], and hybrids (e.g., Q-IT [31,56], Q-TOF [58]) are used increasingly.

2.3. CE–MS for comprehensive analyses

CE has always been touted as a high-resolution technique. In principle, the presence of a fast EOF can make all molecules, regardless of charge, migrate in the same direction and be analyzed simultaneously. In combination with MS as detector, the analytical potential is further enhanced because CE enables temporal separation of components that cannot be mass-differentiated (e.g., isomers), while MS provides a second separation dimension for those which co-migrate. Still, highly complex samples cannot be completely characterized because of instrumental limitations related to dynamic range, and analytical parameters, which generally favor the separation and detection of some compounds over others. At best, simultaneous determination of as many components as possible in a single run can be achieved.

For comprehensive analyses, an attractive approach is to use two or more sets of conditions, which have been optimized for different compound groups, and then concatenate the results. In

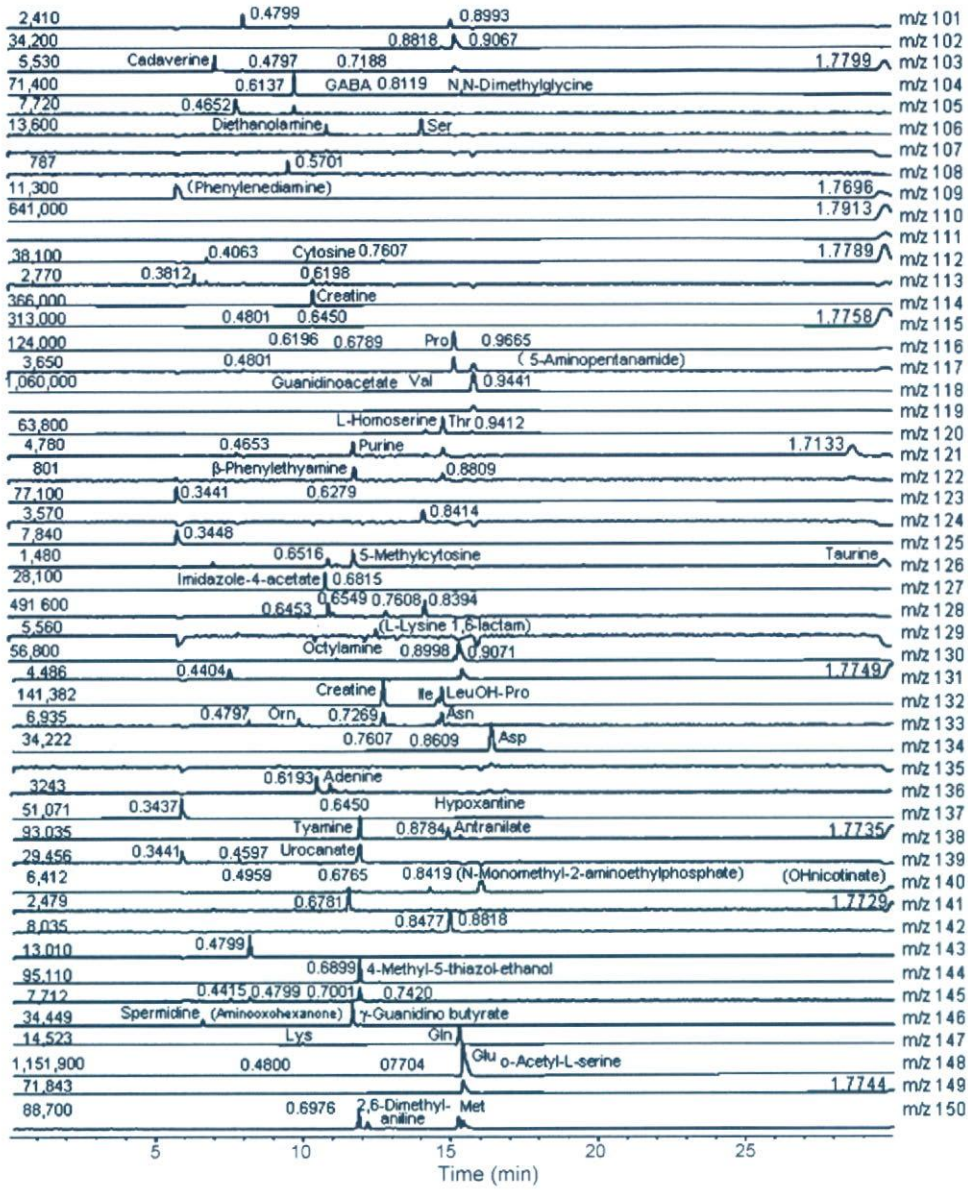

Fig. 3. Selected ion electropherograms for cationic metabolites at $T_{-0.5}$ of B. subtilis 168 in the range of 101–150 *m/z*. The numbers in the upper left corner of each trace are the abundances associated with the tallest peak in the electropherogram, for each *m/z*, and the numbers of tops of peaks are relative migration times normalized with methionine sulfone as internal standard. Reprinted from [79] with permission. Copyright 2003 American Chemical Society.

this manner, wider sample coverage can be obtained, as demonstrated by the works of Soga and colleagues [76,77,79,97]. Amino acids, amines and nucleosides were analyzed as cations using a very low pH electrolyte [54] (Fig. 3). On the other hand, carboxylic acids, phosphorylated carboxylic acids, phosphorylated saccharides, nucleotides, and nicotinamide and flavin adenine coenzymes were analyzed as anions using an alkaline BGS and a cationic polymer-coated capillary (SMILE(+)) to reverse the EOF and prevent deleterious current drops [57]. However, multivalent anions, particularly those of coenzyme A, could not be detected as well-shaped peaks. In a follow-up work [78], they supplanted the SMILE(+)capillary with a neutral capillary in order to prevent anionic species from adsorbing onto the wall, and applied air pressure to the capillary inlet during electrophoresis to provide a constant liquid flow towards the anode. Under these conditions, citrate isomers, nucleotides, dinucleotides, and CoA compounds could be separated and detected well. With a quadrupole mass analyzer, it was necessary to limit the MS scan range to a window of 30 *m/z* in order to maximize detection sensitivity; thus, repeated (33 times, ca. 30 min per run) analysis of the same sample was necessary, requiring as long as 16 h [79]. By switching to a TOF analyzer, however, the number of runs per sample could be reduced to 3 (one for cations, one for anions, one for "nucleotides"). A total of 1692 metabolites from exponentially growing *Bacillus subtilis* cells could be catalogued this way [79] (Fig. 4).

Metabolites are generally identified by matching their migration time and MS or tandem MS spectra against those of pure compounds. However, many metabolite standards are not commercially available (e.g., only 200 of the 600 known

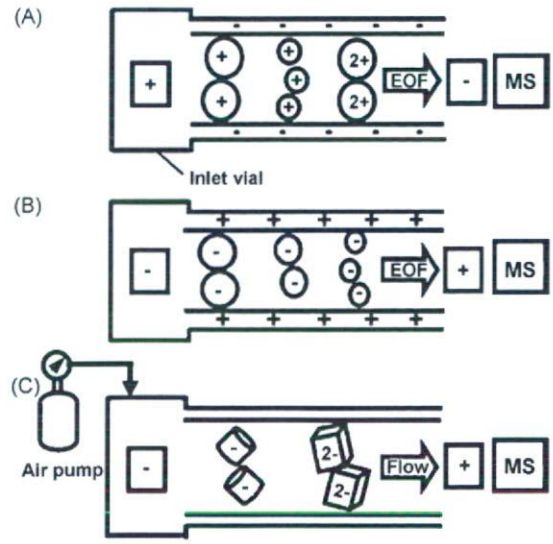

Fig. 4. Schematic of the various CE–MS methods. (A) Cationic metabolites, (B) anionic metabolites, and (C) nucleotides and CoA compounds. Reprinted from [79] with permission. Copyright 2003 American Chemical Society.

yeast metabolites) [8], and metabolomics-specific mass spectral libraries are still limited at this time [7]. For instance, of the 1692 metabolites cited above, only 150 were positively identified and an additional 83 were assigned based on expected charge state and isotopic distribution [79]. For unknown compounds, the use of high-mass accuracy analyzers (e.g., TOF) permit assignment of empirical formulae, while tandem MS enables structural identification via interpretation of their fragmentation patterns. The sheer scale of metabolomics, however, demands novel identification methodologies; as such, computational approaches [21,79,98] are also employed. Sugimoto et al. [98] developed a technique for predicting the identities and migration times of cations in CE–MS using an ensemble of artificial neural networks (ANNs). When evaluated against all metabolites listed in the KEGG (Kyoto Encyclopedia of Genes and Genomes) ligand database, the correct compound among the top three candidates could be predicted in 78.0% of the cases. More recently, Lee et al. [21] reported a method for identifying unknowns by computer modeling of candidate structures to calculate their molecular volumes and intrinsic valence charges, which were subsequently used to estimate their mobilities. Using Simul 5.0 (a freeware), comparisons between predicted and experimental relative migration times of several metabolite candidates gave average relative error under 2%. This strategy enabled differentiation of both isomeric and isobaric amino acid and nucleoside metabolites identified as key nutrients in *E. coli* growth.

For quantitation with ESI–MS, it must be emphasized that most of the uncertainty and potential nonlinearity do not refer to the MS, but rather to the ESI process; thus careful attention has to be given to coupling and separation. An internal standard is the best tool to compensate for changes in ionization efficiency [99].

3. Selected applications

Metabolomic investigations will have strong impact on diverse fields, including genetics, medical science, toxicology, nutrition and agriculture. Their results can be used as chemical basis for taxonomy, to assign functions to genes, identify metabolic intermediates, and elucidate biosynthetic pathways, including novel ones. They can also be used to provide templates for disease diagnosis, or monitor the effects of nutritional and pharmacologic interventions [5]. They can speed the discovery and development of drugs, and to make these drugs safer by predicting the potential for adverse effects earlier [100]. Metabolomics data can be exploited in biotechnology for enhancing the nutritional value of food and engineering of pathways needed for the production of pharmaceuticals in plants [101]. Additionally, they can be applied for assessing the substantial equivalence of genetically modified organisms (GMO) if the metabolic phenotypes of a variety of well-known cultivars, that are commonly believed to be safe, are compared to transgenic plants [102]. Some select applications based on CE–MS are discussed in this section.

3.1. Sample characterization

Several studies involving simple analyses of specific constituents or group of plant principles for which they are valued, were reported [38–41,43,48,75,82,86,103,104], some clearly demonstrating CE as an attractive alternative to LC. Intact, non-desulfated glucosinolates, which have low affinity to reversed phases commonly employed in LC, were analyzed by CE–MS [103]. Using acidic conditions, they were separated and detected as anions, resulting in excellent selectivity and minimal interference from matrix constituents. Additionally, the sensitivity, together with mass accuracy and true isotopic pattern obtainable with TOF-MS, allowed identification of a broad series of glucosinolates in *Arabidopsis thaliana* seeds. Hilz et al. [86] reported better separation of xyloglucan oligosaccharides using CE compared to reversed-phase LC, though separation profiles similar to the former could be obtained by anion exchange chromatography as well. Edwards et al. [82] employed CE–MS for rapid screening of an infusion of aerial parts of *Genista tenera*, a plant used in folk medicine as an antidiabetic agent. At least 26 different phenolic compounds could be distinguished in as short as 10 min, in contrast with a recently reported LC–MS analysis of the same sample where five compounds were separated and identified in 100 min. Furthermore, the use of tandem MS enabled distinction between co-migrating *O*- and *C*-glycosides.

Sato et al. [77] used four independent CE–MS condition tuned for optimum separation and detection of different metabolite classes in the leaves of rice, *Oryza sativa* L. Together with the use of a diode array detector (DAD) almost all water-soluble analytes were determined, and the levels of 88 key metabolites involved in glycolysis, tricarboxylic acid (TCA) cycle, pentose phosphate pathway, photorespiration, and amino acid biosynthesis were measured. Drawing on a similar strategy, Takahashi et al. [105] performed a quantitative comparison of the concentrations of known metabolites, sugars and ions in hygromycin-resistant transgenic rice overexpressing the dihydroflavonol-4-reductase (DFR) gene and transgenic rice with hygromycin-resistant gene alone as control. Differences in the levels of several metabolites, such as *cis*-aconitate, fructose

1,6-bisphosphate, free amino acids, and metals were observed in roots, leaves and seeds, but the concentrations of sugars in seeds were fairly constant.

Carrasco-Pancorbo et al. [49] compared the phenolic contents of different varieties of extra-virgin olive oil. Phenolic compounds in olive oil are acknowledged to be largely responsible for their antioxidant properties, which in turn have been related to their protective effect against chronic and degenerative diseases.

Wahby et al. [88] made the first report about the occurrence of atropine in hemp, *Cannabis sativa*, and determined its concentration, alongside choline, in several transgenic root cultures. Widely varying levels of these compounds were found, and the variations were attributed to differences in plant genotypes, bacterial strains used in inoculation and transformation events. Arráez-Román et al. [80] characterized the methanolic extracts of hop cones, the female flowers of *Humulus lupulus*, which are used for adding flavor and aroma in the beer-brewing process. α-acids were found to be the major components in hops. By analyzing the components present in different extracts, a comparative study of the capacities of different extraction procedures could be carried out. In another work [52], the same group compared the components of different hop varieties before and after natural and forced oxidation in order to determine the best variety as far as storage stability is concerned.

Edwards et al. [56] developed a CE–MS-based method for separation and detection of phosphorylated and acidic metabolites in extracts of *E. coli*, strain DH5-α, enabling 118 compounds to be identified. Interestingly, this figure was higher than those obtained by direct infusion experiments using ESI or MALDI. Li et al. used CE–MS to characterize isomeric LPS of *N. meningitidis* [53] and *Haemophilus influenzae* [106] strains. The occurrence of glycoforms differing by the location or presence of neutral sugar residues was also characterized by tandem MS.

3.2. Elucidating metabolic dynamics

Harada et al. [84] harnessed the usefulness of CE–MS for separation and selective and sensitive detection of underivatized amino acids. ^{15}N-labeled inorganic salts were fed to to *Arabidopsis* (cell line T87) and *Coptis* cultured cells. The ^{15}N labeling ratios of amino acids from T87 cells, cultured under light and dark conditions, at different time points were determined. The rates of increase of the ratios over time were indicative of the length of the pathway for nitrogen incorporation into each amino acid, with most ratios being lower under dark conditions. These results were found to correspond to transcriptional expressions revealed by microarray experiments. In addition, labeling ratios of *Coptis* cultured cells revealed arginine and lysine metabolism inhibition, which should result in inhibition of polyamine biosynthesis and cell division. On the other hand, Tanaka et al. [107] focused on the TCA cycle and its metabolites. The levels of these metabolites in the leaf sheath and leaf blade of transgenic rice expressing the antisense methylmalonate-semialdehyde dehydrogenase, *MMSDH*, were compared to those of control. Results suggested that the concentration of acetyl CoA, the precursor of TCA cycle, is reduced in transgenic rice, and therefore the concentrations of TCA cycle metabolites were altered.

Itoh et al. [108] used CE–MS to perform direct and simultaneous determination of diverse metabolic intermediates for studying the regulation of metabolism *in vitro*. They reconstructed a synthetic *in vitro* glycolysis from ten purified *E. coli* enzymes to obtain a better understanding of the regulation of sequential enzymatic reactions. Their results indicated that the pathway was controlled by a delicate balance between changing metabolite concentrations, and that it behaved like a natural biological oscillating network. Soga et al. [79] employed CE–MS to gain valuable insights into bacterial differentiation and biological events. They profiled *B. subtilis* cells at different time points before and during spore formation stages. Results showed changes in levels of some intermediates in the TCA cycle, such as cis-aconitate, isocitrate, malate, and 2-oxoglutarate, at the end of the exponential growth phase and 2 h thereafter, that were in good agreement with previous findings.

3.3. Assigning functions to genes and proteins

Soo et al. [22] used CE–MS to monitor differences between intracellular pool of sugar nucleotides of parent and isogenic mutants of *Campylobacter jejuni* 81–176. By using product ion scanning, it was possible to determine the precise nature of unexpected sugar nucleotides involved in the biosynthesis of pseudaminic acid. The authors employed sample stacking and obtained as much as 1000-fold increase in sensitivity compared to conventional CE–MS. Additionally, sharper and more resolved peaks were observed under stacking conditions. In a more recent work [109], they used CE–MS in conjunction with hydrophilic interaction liquid chromatography (HILIC)–MS and NMR to investigate the function of flagellin glycosylation genes in *C. jejuni*. They were able to uncover three novel biosynthetic gene functions, completed the structural assignment of two unique glycan-associated intracellular metabolites and demonstrated for the first time *in vivo* a unique interaction between two distinct protein glycosylation pathways.

Saito et al. [76] employed a systematic method based on *in vitro* assays in combination with metabolite profiling to discover novel enzymatic activities. Mixtures of metabolites and candidate proteins were monitored by CE–MS for changes in metabolite composition indicative of the presence of enzymatic activity, while identification of those whose levels changed led to actual substrates and products of reaction. In this way, two proteins from *E. coli*, YbhA and YbiV, were found to display both phosphotransferase and phosphatase activity toward different sugars or sugar phosphates.

3.4. Disease diagnosis and biomarker discovery

Analyses of biofluids, such as urine and blood, can provide important information regarding the metabolic status of an organism. Metabolite concentrations relate to cell and tissue processes, and they reflect both normal variation and toxin- or disease-induced imbalance in single or multiple organ systems

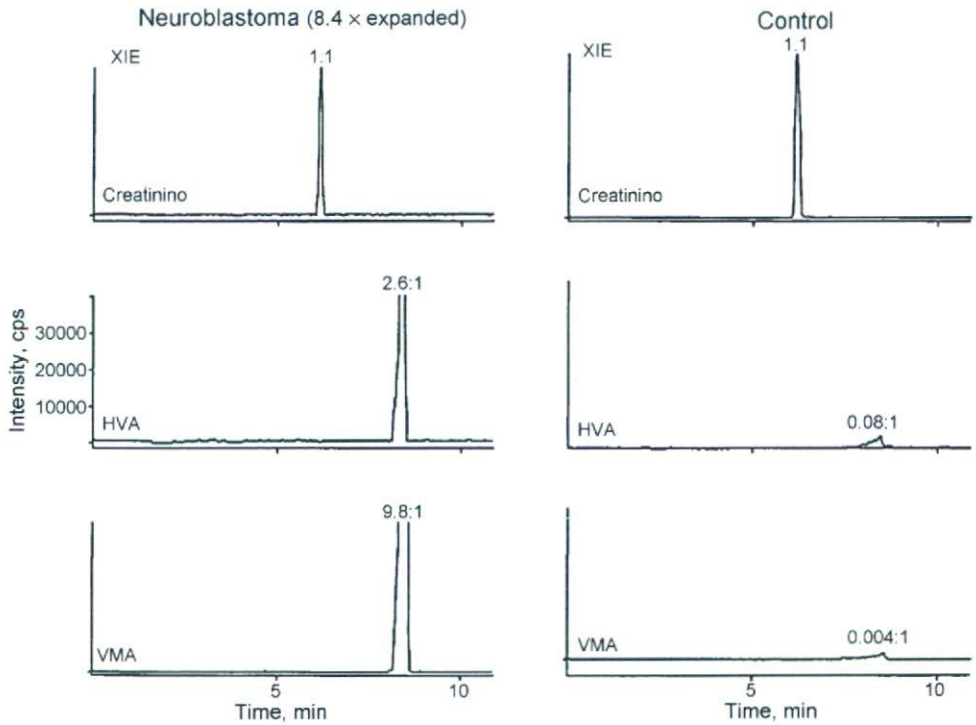

Fig. 5. CE–MS/MS (MRM mode) of a urine sample from a person suffering from neuroblastoma (left) vs. control (right). Reprinted from [90] with permission.

[93]. Some metabolites accumulate as a result of genetic defects causing decreased enzyme activity, thus their abnormally high levels compared to controls can be indicative of diseased conditions, and the information can be used for early detection as well as monitoring progression of a disease. Using CE–MS, it is possible to directly analyze biofluids with minimal pretreatment. Presto Elgstoen et al. [90] described a rapid method for screening for metabolic disorders using urine samples. By using CE–MS/MS in the multiple reaction monitoring (MRM) mode, diagnostic metabolites of several different disorders (e.g., homogentisic acid for alcaptonuria, homovanillic acid (HVA) and vanillylmandelic acid (VMA) for neuroblastoma (Fig. 5), C_{12} and C_{14} epoxy acids for Zellweger syndrome) could be identified. Schultz and Moini [59] applied the technique they developed for analysis of underivatized amino acids in the detection of abnormally elevated levels of phenylalanine and tyrosine in the blood of newborns suffering from phenylketonurea (PKU) and tyrosinemia, respectively.

Ullsten et al. [93] reported a fast and general method for metabolic profiling of urine, combining CE–MS with multi-

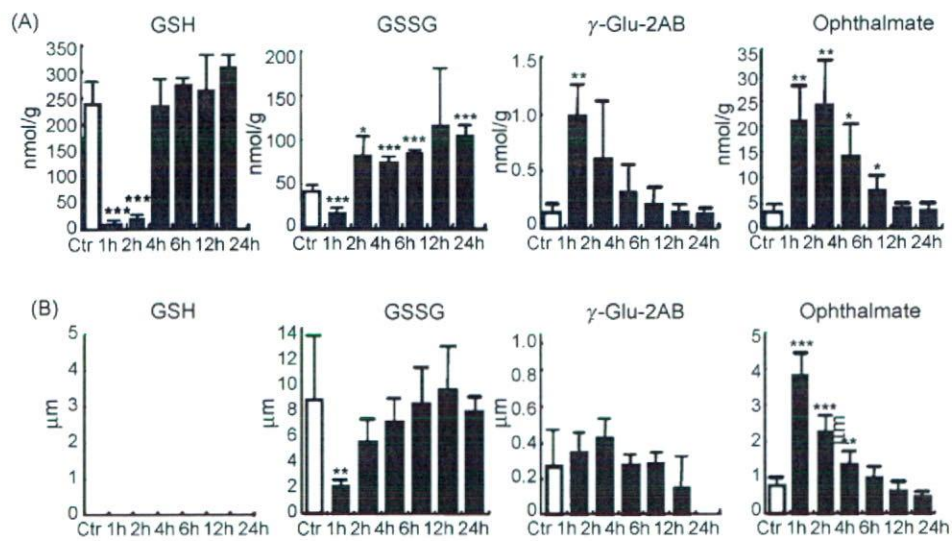

Fig. 6. Changes in metabolite levels in (A) mouse liver and (B) serum 1, 2, 4, 6, 12, and 24 h after acetaminophen (AAP) treatment ($n = 4$). *Asterisks* indicate significant differences (***, $p < 0.001$; **, $p < 0.01$; *, $p < 0.05$. The hepatic glutathione (GSH) level at 1 h after AAP treatment was ~28 times lower than in the controls ($p < 1.6 \times 10^{-5}$). On the other hand, the ophthalmate level in mouse serum at 1 h after AAP treatment increased ~5-fold compared with the controls ($p = 0.0001$). Reprinted from [97].

variate data analysis. Urine profiles before and after intake of paracetamol could be differentiated, and the *m/z* values of the compounds responsible for the differentiation could be pinpointed. However, since these compounds were not definitively identified, it was not possible to ascribe biological significance to those correlated to ingestion of paracetamol. In contrast, Soga et al. [97] developed a differential display tool with identification capability. Serum and liver extracts of mice before and after acetaminophen-induced hepatotoxicity were profiled by CE–MS, and changes in metabolite profiles, including their levels, were highlighted. In this manner, activation of ophthalmate biosynthesis pathway was revealed, and serum ophthalmate was shown to be a sensitive indicator of hepatic glutathione depletion, and thus, may be a new biomarker for oxidative stress (Fig. 6).

3.5. Assessing food safety

The potential for changes in the level of natural toxicants that could result from metabolic processes associated with uptake, biosynthesis and transport of nutritional components, is considered critical in determining the overall risk for food derived from genetically modified plants [39]. Bianco et al. [39] used NACE-MS to compare the steroidal glycoalkaloid (GA) content of transgenic tubers of potato plants, virus Y-resistant, intermediate, susceptible, and control (var. Desiree), and found no statistically significant differences among them. GAs are a class of toxicants involved in the chemical defense of plants, acting as nonspecific protectors or repellents against potential pest predators. They are not destroyed by typical food processing, thus, it is important to monitor their levels in tubers intended for human consumption.

4. Conclusions and future outlook

From the technological viewpoint, metabolomics is a very demanding field. Currently, an "ideal" analytical platform does not exist, and it is unlikely that there will be one in the future. However, continuous improvements in instrumentation that increase the throughput, robustness, sensitivity and accuracy of present methods, in addition to the development of automated tools for processing huge amounts of data, can be expected to expand sample coverage.

Different methodologies have distinct advantages that can be exploited in investigating different metabolite classes, and the resulting information put together to obtain better characterization of the metabolome; thus, the importance of complementary approaches. In this regard, CE–MS definitely has a place in metabolomics research. Though reports up to this time are far outnumbered by GC–MS- and LC–MS-based ones, and most of these deal with targeted rather than comprehensive metabolite analyses, its usefulness for polar analytes has been clearly demonstrated. With the availability of APPI as MS interface, which is able to generate ions from nonpolar compounds and also extend the range of MS-compatible buffer components and additives, CE–MS will be more broadly applicable.

References

[1] S.G. Oliver, M.K. Winston, D.B. Kell, F. Baganz, Trends Biotechnol. 16 (1998) 373.
[2] R. Goodacre, S. Vaidyanathan, W.B. Dunn, G.G. Harrigan, D.B. Kell, Trends Biotechnol. 22 (2004) 245.
[3] Q.-Z. Wang, C.-Y. Wu, T. Chen, X. Chen, X.-M. Zhao, Appl. Microbiol. Biotechnol. 70 (2006) 151.
[4] C. Birkemeyer, A. Luedemann, C. Wagner, A. Erban, J. Kopka, Trends Biotechnol. 23 (2005) 28.
[5] K. Dettmer, P.A. Aronov, B.D. Hammock, Mass Spectrom. Rev. 26 (2007) 51.
[6] S.G. Villas-Bôas, S. Mas, M. Åkesson, J. Smedsgaard, J. Nielsen, Mass Spectrom. Rev. 24 (2004) 613.
[7] W.B. Dunn, D.I. Ellis, Trends Anal. Chem. 24 (2005) 285.
[8] W.B. Dunn, N.J.C. Bailey, H.E. Johnson, Analyst 130 (2005) 606.
[9] J. Nielsen, S. Oliver, Trends Biotechnol. 23 (2005) 544.
[10] Z. Yang, J. Pharm. Biomed. Anal. 40 (2006) 516.
[11] R.D. Hall, New Phytol. 169 (2006) 453.
[12] J. Dallüge, J. Beens, U.A.Th. Brinkman, J. Chromatogr. A 1000 (2003) 69.
[13] M.Z. Özel, Anal. Bioanal. Chem. 382 (2005) 115.
[14] R.M.M. Perera, P.J. Marriott, I.E. Galbally, Analyst 127 (2002) 1601.
[15] J.E. MacNair, K.C. Lewis, J.W. Jorgenson, Anal. Chem. 69 (1997) 983.
[16] Y. Shen, R. Zhang, R.J. Moore, J. Kim, T.O. Metz, K.K. Hixson, R. Zhao, E.A. Livesay, H.R. Udseth, R.D. Smith, Anal. Chem. 77 (2005) 3090.
[17] I.D. Wilson, J.K. Nicholson, J. Castro-Perez, J.H. Granger, K.A. Johnson, B.W. Smith, R.S. Plumb, J. Proteome Res. 4 (2005) 591.
[18] M. Tomita, T. Nishioka (Eds.), Metabolomics: The Frontier of Systems Biology, Springer, Tokyo, 2005.
[19] P. Britz-McKibbin, M.J. Markuszewski, T. Iyanagi, K. Matsuda, T. Nishioka, S. Terabe, Anal. Biochem. 313 (2003) 89.
[20] L. Jia, B.F. Liu, S. Terabe, T. Nishioka, Anal. Chem. 76 (2004) 1419.
[21] R. Lee, A.S. Ptolemy, L. Niewczas, P. Britz-McKibbin, Anal. Chem. 79 (2007) 403.
[22] E.C. Soo, A.J. Aubry, S.M. Logan, P. Guerry, J.F. Kelly, N.M. Young, P. Thibault, Anal. Chem. 76 (2004) 619.
[23] K. Isoo, S. Terabe, Anal. Chem. 75 (2004) 6789.
[24] S.R. Bean, G.L. Lookhart, J.A. Bietz, J. Agric. Food Chem. 48 (2000) 318.
[25] D.W. Armstrong, G. Schulte, J.M. Schneiderheinze, D.J. Westenberg, Anal. Chem. 71 (1999) 5465.
[26] Y. Ishihama, H. Katayama, N. Asakawa, Anal. Biochem. 287 (2000) 45.
[27] H. Ozaki, N. Itou, S. Terabe, Y. Takada, M. Sakairi, H. Koizumi, J. Chromatogr. A 716 (1995) 69.
[28] K. Koezuka, H. Ozaki, N. Matsubara, S. Terabe, J. Chromatogr. B 689 (1997) 3.
[29] M. Frommberger, P. Schmitt-Kopplin, F. Menzinger, V. Albrecht, M. Schmid, L. Eberl, A. Hartmann, A. Kettrup, Electrophoresis 24 (2003) 3067.
[30] J.C.M. Waterval, H. Lingeman, A. Bult, W.J.M. Underberg, Electrophoresis 21 (2000) 4029.
[31] F.-Y. Che, J.-F. Song, R. Zeng, K.-Y. Wang, Q.-C. Xia, J. Chromatogr. A 858 (1999) 229.
[32] M. Larsson, R. Sundberg, S. Folestad, J. Chromatogr. A 934 (2001) 75.
[33] A.S. Ptolemy, P. Britz-McKibbin, Analyst 130 (2005) 1263.
[34] A.S. Ptolemy, M. Le Bihan, P. Britz-McKibbin, Electrophoresis 26 (2005) 4206.
[35] A.S. Ptolemy, L. Tran, P. Britz-McKibbin, Anal. Biochem. 354 (2006) 192.
[36] M.-L. Riekkola, Electrophoresis 23 (2002) 3865.
[37] I. Bjørnsdottir, J. Tjornelund, H. Hansen, Electrophoresis 19 (1998) 2179.
[38] G. Bianco, P. Schmitt-Kopplin, G. De Benedetto, A. Kettrrup, T.R.I. Cataldi, Electrophoresis 23 (2002) 2904.
[39] G. Bianco, P. Schmitt-Kopplin, A. Crescenzi, S. Comes, A. Kettrup, T.R.I. Cataldi, Anal. Bioanal. Chem. 375 (2003) 799.
[40] S. Sturm, E.-M. Strasser, H. Stuppner, J. Chromatogr. A 1112 (2006) 331.

[41] M. Unger, M. Dreyer, S. Specker, S. Laung, M. Pelzing, C. Neuseüss, U. Holzgrabe, G. Bringmann, Phytochem. Anal. 15 (2004) 21.
[42] K. Vuorensola, H. Siten, R. Kostiainen, T. Kotiaho, J. Chromatogr. A 979 (2002) 179.
[43] J. Ding, P. Vouros, Anal. Chem. 71 (1999) 378A.
[44] J. Žídková, J. Chmelík, J. Mass Spectrom. 36 (2001) 417.
[45] J. Cabálková, J. Židková, L. Přibyla, J. Chmelík, Electrophoresis 25 (2004) 487.
[46] H.M. Liebich, S. Müller-Hagedorn, F. Klaus, K. Meziane, K.-R. Kim, A. Frickenschmidt, B. Kammerer, J. Chromatogr. A 1071 (2005) 271.
[47] J.L. Edwards, R.T. Kennedy, Anal. Chem. 77 (2005) 2201.
[48] D. Arráez-Román, A.M. Gómez-Caravaca, M. Gómez-Romero, A. Segura-Carretero, A. Fernández-Gutiérrez, J. Pharm. Biomed. Anal. 41 (2006) 1648.
[49] A. Carrasco-Pancorbo, D. Arráez-Román, A. Segura-Carretero, A. Fernández-Gutiérrez, Electrophoresis 27 (2006) 2182.
[50] A.V. Colnaghi Simionato, C. Simó, A. Cifuentes, P. Teixeira Lacava, W.L. Araújo, J.L. Azevedo, E. Carrilho, Electrophoresis 27 (2006) 2567.
[51] S. Duteil, P. Gareil, S. Girault, A. Mallet, C. Feve, L. Siret, Rapid Commun. Mass Spectrom. 13 (1999) 1889.
[52] R. García-Villalba, S. Cortacero-Ramírez, A. Segura-Carretero, J.A. Martín-Lagos Contreras, A. Fernández-Gutiérrez, J. Agric. Food Chem. 54 (2006) 5400.
[53] J. Li, A.D. Cox, D. Hood, E.R. Moxon, J.C. Richards, Electrophoresis 25 (2004) 2017.
[54] T. Soga, D.N. Heiger, Anal. Chem. 72 (2000) 1236.
[55] L. Ge, J.W.H. Yong, S.N. Tan, E.S. Ong, Electrophoresis 27 (2006) 2171.
[56] J.L. Edwards, C.N. Chisolm, J.G. Shackman, R.T. Kennedy, J. Chromatogr. A 1106 (2006) 80.
[57] T. Soga, Y. Ueno, H. Naraoka, Y. Ohashi, M. Tomita, T. Nishioka, Anal. Chem. 74 (2002) 2233.
[58] A. Zamfir, D.G. Seidler, E. Schönherr, H. Kresse, J. Peter-Katalinić, Electrophoresis 25 (2004) 2010.
[59] C.L. Schultz, M. Moini, Anal. Chem. 75 (2003) 1508.
[60] R.B. Cole (Ed.), Electrospray Ionization Mass Spectrometry, Wiley, New York, 1997.
[61] S.L. Nilsson, C. Andersson, P.J.R. Sjöberg, D. Bylund, P. Petersson, M. Jörntén-Karlsson, K.E. Markides, Rapid Commun. Mass Spectrom. 17 (2003) 2267.
[62] Y. Takada, M. Sakairi, H. Koizumi, Rapid Commun. Mass Spectrom. 9 (1995) 488.
[63] K. Isoo, K. Otsuka, S. Terabe, Electrophoresis 22 (2001) 3426.
[64] S.J. Bos, S.M. van Leeuwen, U. Karst, Anal. Bioanal. Chem. 384 (2006) 85.
[65] Y. Hsieh, K. Merkle, G. Wang, J.-M. Brisson, W.A. Korfmacher, Anal. Chem. 75 (2003) 3122.
[66] D.B. Robb, T.R. Covey, A.P. Bruins, Anal. Chem. 72 (2000) 3653.
[67] K.A. Hanold, S.M. Fischer, P.H. Cormia, C.E. Miller, J.A. Syage, Anal. Chem. 76 (2004) 2842.
[68] J.A. Starkey, Y. Mechref, J. Muzikar, W.J. McBride, M.V. Novotny, Anal. Chem. 78 (2006) 3342.
[69] D.B. Robb, M.W. Blades, Anal. Chem. 78 (2006) 8162.
[70] R. Mol, G.J. de Jong, G.W. Somsen, Electrophoresis 26 (2005) 146.
[71] R. Mol, G.J. de Jong, G.W. Somsen, Anal. Chem. 77 (2005) 5277.
[72] E.J. Want, A. Nordstrom, H. Morita, G. Siuzdak, J. Proteome Res. 6 (2007) 459.
[73] S.K. Johnson, L.L. Houk, D.C. Johnson, R.S. Houk, Anal. Chim. Acta 389 (1999) 1.
[74] C.C. Liu, J.S. Huang, D.L.J. Tyrrell, N.J. Dovichi, Electrophoresis 26 (2005) 1424.
[75] L. Mateus, S. Cherkaoui, P. Christen, J.-L. Veuthey, Electrophoresis 20 (1999) 3402.
[76] N. Saito, M. Robert, S. Kitamura, R. Baran, T. Soga, H. Mori, T. Nishioka, M. Tomita, J. Proteome Res. 5 (2006) 1979.
[77] S. Sato, T. Soga, T. Nishioka, M. Tomita, Plant J. 40 (2004) 151.
[78] T. Soga, Y. Ueno, H. Naraoka, K. Matsuda, M. Tomita, T. Nishioka, Anal. Chem. 74 (2002) 6224.
[79] T. Soga, Y. Ohashi, Y. Ueno, H. Naraoka, M. Tomita, T. Nishioka, J. Proteome Res. 2 (2003) 488.
[80] D. Arráez-Román, S. Cortacero-Ramírez, A. Segura-Carretero, J.-A. Martín-Lagos Contreras, A. Fernández-Gutiérrez, Electrophoresis 27 (2006) 2197.
[81] L. Behndahl, B. Gammelgaard, J. Anal. At. Spectrom. 19 (2004) 950.
[82] E.L. Edwards, J.A. Rodrigues, J. Ferreira, D.M. Goodall, A.P. Rauter, J. Justino, J. Thomas-Oates, Electrophoresis 27 (2006) 2164.
[83] K. Harada, E. Fukusaki, A. Kobayashi, J. Biosci. Bioeng. 101 (2006) 403.
[84] K. Harada, E. Fukusaki, T. Bamba, F. Sato, A. Kobayashi, Biotechnol. Prog. 22 (2006) 1003.
[85] T. He, D. Quinn, E. Fu, Y.K. Wang, J. Chromatogr. B 727 (1999) 43.
[86] H. Hilz, L.E. de Jong, M.A. Kabel, H.A. Schols, A.G.J. Voragen, J. Chromatogr. A 1133 (2006) 275.
[87] A.V. Kühn, H.H. Rüttinger, R.H.H. Neubert, K. Raith, Rapid Commun. Mass Spectrom. 17 (2003) 576.
[88] I. Wahby, D. Arráez-Román, A. Segura-Carretero, F. Ligero, J.M. Caba, A. Fernández-Gutiérrez, Electrophoresis 27 (2006) 2208.
[89] U. Warnke, C. Rappel, H. Meier, C. Kloft, M. Galanski, C.G. Hartinger, B.K. Keppler, U. Jaehde, Chem. Biochem. 5 (2004) 1543.
[90] K.B. Presto Elgstoen, J.Y. Zhao, J.F. Anacleto, E. Jellum, J. Chromatogr. A 914 (2001) 265.
[91] J. Hau, S. Devaud, I. Blank, Electrophoresis 25 (2004) 2077.
[92] T. Soga, Y. Kakazu, M. Robert, M. Tomita, T. Nishioka, Electrophoresis 25 (2004) 1964.
[93] S. Ullsten, R. Danielsson, D. Bäckström, P. Sjöberg, J. Berquist, J. Chromatogr. A 1117 (2006) 87.
[94] K. Vuorensola, J. Kokkonen, H. Sirén, R.A. Ketola, Electrophoresis 22 (2001) 4347.
[95] Z.D. Peterson, M.L. Lee, S.W. Graves, J. Chromatogr. B 810 (2004) 101.
[96] Z.D. Peterson, D.C. Collins, C.R. Bowerbank, M.L. Lee, S.W. Graves, J. Chromatogr. B 776 (2002) 221.
[97] T. Soga, R. Baran, M. Suematsu, Y. Ueno, S. Ikeda, T. Sakurakawa, Y. Kakazu, T. Ishikawa, M. Robert, T. Nishika, M. Tomita, J. Biol. Chem. 281 (2006) 16768.
[98] M. Sugimoto, S. Kikuchi, M. Arita, T. Soga, T. Nishioka, M. Tomita, Anal. Chem. 77 (2005) 78.
[99] J. Ohnesorge, C. Neuseüss, H. Wätzig, Electrophoresis 26 (2005) 3973.
[100] L. Bren, FDA Consumer Magazine 39 (2005) 28.
[101] G. Giddings, G. Allison, D. Brooks, A. Carter, Nat. Biotechnol. 18 (2000) 1151.
[102] R. Bhalla, K. Narasimhan, S. Swarup, Plant Cell Rep. 24 (2005) 562.
[103] G. Bringmann, I. Kajahn, C. Neuseüss, M. Pelzing, S. Laug, M. Unger, U. Holzgrabe, Electrophoresis 26 (2005) 1513.
[104] E. von Roepenack-Lahaye, T. Degenkolb, M. Zerjeski, M. Franz, U. Roth, L. Wessjohann, J. Schmidt, D. Scheel, S. Clemens, Plant Physiol. 134 (2005) 548.
[105] H. Takahashi, M. Hayashi, F. Goto, S. Sato, T. Soga, T. Nishioka, M. Tomita, M. Kawai-Yamada, H. Uchimiya, Ann. Bot. 98 (2006) 819.
[106] J. Li, A.D. Cox, D.W. Hood, E.L.K. Schweda, E.R. Moxon, J.C. Richards, Mol. Biosyst. 1 (2005) 46.
[107] N. Tanaka, H. Takahashi, H. Kitano, M. Matsuoka, S. Akao, H. Uchimiya, S. Komatsu, J. Proteome Res. 4 (2005) 1575.
[108] A. Itoh, Y. Ohashi, T. Soga, H. Mori, T. Nishioka, M. Tomita, Electrophoresis 25 (2004) 1996.
[109] D.J. McNally, J.P.M. Hui, A.J. Aubry, K.K.K. Mui, P. Guerry, J.-R. Brisson, S.M. Logan, E.C. Soo, J. Biol. Chem. 281 (2006) 18489.

Available online at www.sciencedirect.com
ScienceDirect
Journal of Chromatography A, 1159 (2007) 134–141
JOURNAL OF CHROMATOGRAPHY A
www.elsevier.com/locate/chroma

Direct measurement of isotopomer of intracellular metabolites using capillary electrophoresis time-of-flight mass spectrometry for efficient metabolic flux analysis

Yoshihiro Toya [a,b], Nobuyoshi Ishii [a,b], Takashi Hirasawa [a], Miki Naba [a], Kenta Hirai [a], Kaori Sugawara [a], Saori Igarashi [a], Kazuyuki Shimizu [a,c], Masaru Tomita [a,b], Tomoyoshi Soga [a,b,*]

[a] *Institute for Advanced Biosciences, Keio University, 403-1 Nipponkoku, Daihoji, Tsuruoka, Yamagata 997-0017, Japan*
[b] *Systems Biology Program, Graduate School of Media and Governance, Keio University, 5322 Endo, Fujisawa, Kanagawa 252-8520, Japan*
[c] *Department of Bioscience and Bioinformatics, Kyushu Institute of Technology, 680-4 Kawazu, Iizuka, Fukuoka 820-8502, Japan*

Available online 13 April 2007

Abstract

We have developed a metabolic flux analysis method that is based on ^{13}C-labeling patterns of the intracellular metabolites directly measured by capillary electrophoresis time-of-flight mass spectrometry (CE–TOFMS). The flux distribution of the central carbon metabolism in *Escherichia coli* was determined by this new approach and the results were compared with findings obtained by conventional GC–MS analysis based on isotopomer of the proteinogenic amino acids. There were some differences in estimation results between new approach using CE–TOFMS and conventional approach using GC–MS. These were thought to be attributable to variations in measured mass distributions between amino acids and the corresponding precursors and to differences in the sensitivity of the exchange coefficients to mass distributions. However, our CE–TOFMS method facilitates high-throughput flux analysis without requiring complicated sample preparation such as hydrolysis of proteins and derivatization of amino acids.

Keywords: Metabolic flux analysis; ^{13}C-labeling experiment; CE–TOFMS; GC–MS; Exchange coefficient

1. Introduction

Bio-oriented chemicals and fuels such as ethanol, lactate, and succinate, mainly produced by microorganisms, have recently gained attention. To increase the productivity of these useful compounds, the cell physiology and the metabolic flow and regulation involved in the synthesis of the target products must be understood. However, the complexity of metabolic networks hampers elucidation of the regulatory mechanisms of the cellular metabolism.

Metabolic flux analysis (MFA), a powerful method for the quantitative estimation of the intracellular flux for each metabolic reaction that cannot be observed directly, facilitates understanding of the cellular physiology and of metabolic regulatory mechanisms. MFA studies for the microorganisms such as bacteria, yeast, and fungi as well as plants and animal cells have been reported [1–5].

MFA that employs ^{13}C-labeling can address complex biological networks consisting of cyclic, parallel, and reversible reactions because information on the metabolism of the ^{13}C-labeled carbon source through intracellular metabolic pathways is evident from the labeling patterns of the cellular compounds. Thus, the flux distribution of the metabolic reactions can be estimated from the labeling patterns of the appropriate compounds. In the conventional MFA protocols, proteinogenic amino acids are used as the compounds to determine for the labeling patterns. After a biomass hydrolysate is obtained from cells grown in the presence of a ^{13}C-labeled carbon source, the labeled substrates incorporated into the cells are metabolized to amino acids through the metabolic pathways and the labeling patterns of proteinogenic amino acids are measured by GC–MS and/or NMR spectroscopy [6,7].

Although ^{13}C-labeling-based MFA has been employed in many applications, it presents at least two major problems. First, the method is usually applied only in steady-state continuous cultures; it cannot be applied to assess biologically or industrially important batch and fed-batch cultures. Since MFA is

* Corresponding author. Tel.: +81 235 29 0528; fax: +81 235 29 0574.
E-mail address: soga@sfc.keio.ac.jp (T. Soga).

0021-9673/$ – see front matter © 2007 Elsevier B.V. All rights reserved.
doi:10.1016/j.chroma.2007.04.011

based on the labeling patterns of proteinogenic amino acids, it is difficult to estimate the flux distribution under non-steady-state conditions [8]. Second, the method is inconvenient with respect to measurements and sample preparation for GC–MS and NMR. The low sensitivity of NMR requires a large amount of sample and optimization of measurement conditions is difficult; GC–MS, on the other hand, requires derivatization procedures prior to analysis because almost all intracellular metabolites are nonvolatile. To overcome these problems, the direct measurement of low molecular weight (MW) metabolites by LC–MS has been attempted. van Winden et al. [9] used an LC–MS method to analyze metabolites; they used a mass isotopomer to assess flux distribution in the glycolysis of yeast cells. However, as the condition settings for LC–MS strongly depend on empirical rules, increasing the measurable metabolites is a time-consuming task.

Metabolomics, which can be defined as the measurement of the level of all intracellular metabolites, is an emerging tool that can be used not only to gain insight into cellular function but also to investigate human diseases and to discover biomarkers, and in the metabolic engineering of microorganisms and plants [10–12]. Capillary electrophoresis mass spectrometry (CE–MS), a novel metabolomics technology, has become a powerful tool for the global analysis of charged metabolites. The major advantages of CE–MS are its extremely high resolution and its ability to analyze directly almost any charged species [13]. Our group has developed a new metabolome analysis method using capillary electrophoresis time-of-flight mass spectrometry (CE–TOFMS) [10]. On average, our technique improved sensitivity several-fold; improvement was as much as 65-fold higher values obtained with conventional capillary electrophoresis quadrupole mass spectrometry. In addition, CE–TOFMS yielded high-throughput quantitative analysis and exact (milli) mass level differentiation.

Here we propose a new MFA method using CE–TOFMS for the acquisition of labeling information, i.e. the mass distribution, of intracellular low MW metabolites. Using CE–TOFMS, we obtained the labeling patterns of metabolic intermediates of the main metabolic pathways in *E. coli* including glycolysis, the tricarboxylic acid (TCA) cycle, and the pentose phosphate pathway and anaplerotic pathway. Using the mass distribution data of intracellular metabolites or proteinogenic amino acids we determined the flux distribution in the investigated pathways and compared the results obtained by the two methods.

2. Experimental

2.1. E. coli strains, culture condition, and media

For ^{13}C-labeling, we performed a glucose-limited chemostat culture of the wild-type *E. coli* BW25113 (*lacI*^{q} *rrnB*$_{T14}$ Δ*lacZ*$_{WJ16}$ *hsdR514* Δ*araBAD*$_{AH33}$ Δ*rhaBAD*$_{LD78}$) using a synthetic medium (48 mM Na_2HPO_4, 22 mM KH_2PO_4, 10 mM NaCl, 45 mM $(NH_4)_2SO_4$, 4 g/l glucose) supplemented with 1 mM $MgSO_4$, 1 mg/ml thiamine, 0.056 mg/l $CaCl_2$, 0.08 mg/l $FeCl_3$, 0.01 mg/l $MnCl_2{\cdot}4H_2O$, 0.017 mg/l $ZnCl_2$, 0.0043 mg/l $CuCl_2{\cdot}2H_2O$, 0.006 mg/l $CoCl_2{\cdot}2H_2O$, and 0.06 mg/l $Na_2MoO_4{\cdot}2H_2O$. The dilution rates of the chemostat culture were set at 0.1 and 0.5 h^{-1}. Cultivation was carried out at 37 °C in a working volume of 1 l in a 2 l BMJ02-PI reactor (Able, Tokyo, Japan) equipped with pH, dissolved oxygen concentration, and temperature sensors. The O_2 and CO_2 concentrations in off-gas were monitored using Offgas analyzer (DEX-2562, Able). The airflow rate was kept at 1 l/min and the pH was maintained at 7.0 by the automatic addition of HCl or NaOH throughout the cultivation.

2.2. ^{13}C-labeling

^{13}C-labeling was started after confirming the steady state of the chemostat culture based on the CO_2 production rate and the cell concentration. The feed medium containing 4 g/l of naturally labeled glucose was replaced with the same medium containing 0.8 g/l of [1-^{13}C] glucose, 0.8 g/l of [U-^{13}C] glucose and 2.4 g/l of naturally labeled glucose. Samples for CE–TOFMS analysis and biomass samples for GC–MS analysis were obtained after two residence times.

2.3. Measurement of extracellular metabolites concentration

To determine the extracellular fluxes, the concentration of extracellular metabolites such as ethanol, D-lactate, acetate, formate, succinate, pyruvate, and glucose was measured using an enzymatic assay kit (F-kit, Roche Diagnostics).

2.4. GC–MS analysis

The biomass sample obtained from 250 ml of culture was suspended in about 4 ml of 6 M HCl and then hydrolyzed at 105 °C for 16 h. After cooling, HCl was evaporated with a centrifugal evaporator (CVE-3100, Tokyo Rikakikai Co., Ltd., Japan). The dried hydrolysate was resuspended in water and then filtrated through a 0.22-μm pore size filter (Millipore Co., USA). The filtrate was dried again and redissolved in 1.5 ml of acetonitrile. For derivatization, the resulting 80 μl of biomass hydrolysate dissolved in acetonitrile was mixed with an equal volume of *N*-methyl-*N*-(*tert*-butyldimethylsilyl)-trifluoroacetamide and then incubated at 110 °C for 30 min. After cooling, the derivatized sample was subjected to GC–MS analysis on a TruboMass Gold mass spectrometer (Perkin-Elmer, USA). We monitored the fragment ions $[M-57]^+$ and $[M-159]^+$ of *tert*-butyldimethylsilylated (TBDMS-) amino acids (Ala, Gly, Val, Ile, Pro, Met, Phe, Asp, Glu and Tyr). The analytical conditions for GC–MS were described elsewhere [14].

2.5. CE–TOFMS analysis

10 ml of *E. coli* chemostat culture was passed through a 0.45-μm pore size filter (Millipore). The *E. coli* cells on the filter were washed with 20 ml of Milli-Q water, plunged into 4 ml of methanol containing 2 μM 2-(*N*-morpholino)ethanesulfonic acid, 2 μM trimesate, 2 μM methionine sulfone and 2 μM 3-aminopyrrolidine as internal standard. Then, 4 ml of chloroform

and 1.6 ml of Milli-Q water were added to the solution and the mixture was thoroughly mixed. The solution was centrifuged at 2300 × *g* for 5 min at 4 °C, and the separated methanol layer was centrifugally filtered through a Millipore 5-kDa cutoff filter to remove high MW compounds. The filtrate was lyophilized and then dissolved in 20 μl of Milli-Q water before CE–TOFMS analysis. All CE–TOFMS experiments were performed using an Agilent CE capillary electrophoresis system (Agilent Technologies, Germany), an Agilent G3250AA LC/MSD TOF system (Agilent Technologies, Palo Alto, CA), an Agilent1100 series binary HPLC pump, the G1603A Agilent CE–MS adapter and G1607 Agilent CE–ESI-MS sprayer kit. The analytical conditions for CE–TOFMS were described elsewhere [10].

2.6. Metabolic flux analysis

For MFA, we constructed the stoichiometric reaction model of the main metabolic pathway including glycolysis, the pentose phosphate pathway, the TCA cycle, the anaplerotic pathway, and the glyoxylate shunt (see Appendix A).

To circumvent the difficulties involved in the numerical treatment of high exchange fluxes, non-linear mapping between the exchange flux and exchange coefficient was employed for bidirectional reactions such as,

$$v_k^{\mathrm{exch}} = \frac{\mathrm{exch}_k}{1 - \mathrm{exch}_k} \times \beta \tag{1}$$

where v_k^{exch} and exch_k represent the exchange flux and exchange coefficient for reaction v_k, respectively [15]. The value of 100 was used for β in the present study. Flux estimation was carried out using the modified method described by Zhao and Shimizu [16]. In our MFA protocol, three free fluxes (v_2, v_{10}, v_{25}), seven exchange coefficients (exch_2, exch_7, exch_{13}, exch_{14}, exch_{15}, exch_{22}, exch_{23}) and extracellular fluxes were optimized by determining the mass distributions iteratively computed from the assumed fluxes as the best fit to the measured mass distributions of intracellular metabolites or amino acids, using global search algorithms such as the genetic algorithm. The optimizing function was defined as

$$\min J = \sum_{i=1}^{N} \left(\mathrm{MDV}_i^{\mathrm{measured}} - \mathrm{MDV}_i^{\mathrm{simulated}} \right)^2 + \sum_{j=1}^{M} \left(r_j^{\mathrm{measured}} - r_j^{\mathrm{simulated}} \right)^2 \tag{2}$$

where $\mathrm{MDV}_i^{\mathrm{measured}}$ is the mass distribution of the *i*th measured substance, $\mathrm{MDV}_i^{\mathrm{simulated}}$ the simulated mass distribution of the corresponding substance, and N the number of measured substances, r_j^{measured} the measured extracellular metabolite or biomass synthesis flux for *j*th reaction, $r_j^{\mathrm{simulated}}$ the simulated extracellular metabolite or biomass synthesis flux for corresponding reaction, and M the number of the reactions for extracellular metabolite or biomass synthesis fluxes. Biomass synthesis fluxes were obtained from specific growth rate and biomass content [17]. The overall flux distributions were calculated from the estimated free fluxes and exchange coefficients. The optimized flux was selected from the results obtained by 100 independent flux estimations using a single mass distribution data set of intracellular metabolites or amino acids, respectively, at each specific growth rate. Moreover, at the specific growth rate 0.5 h^{-1}, the glyoxylate shunt was omitted from the reaction model as its activity was previously shown to be negligible at such high growth rates [18].

In the new MFA method, we used the mass distributions of intracellular metabolites measured by CE–TOFMS. For comparison purposes, we also used the mass distributions of the proteinogenic amino acids measured by GC–MS. The mass distributions of the measured substances were corrected, according to the method of reported by van Winden et al. [19], taking the natural isotope abundances of C, H, O, N, P, S, and Si atoms into account. Additionally, further correction in mass distributions of proteinogenic amino acids was performed, to achieve isotopic steady state by the method of Dauner et al. [20]. The correction in mass distributions of intracellular metabolites for achievement of isotopic steady state is not necessary, because the pool sizes of intracellular metabolites are smaller than those of proteinogenic amino acids [20]. All calculations were carried out with MATLAB 7.1 with the Genetic Algorithm and Direct Search Toolbox 2.0.1 (Mathworks Inc., USA).

2.7. Sensitivity analysis for changes in the exchange coefficient

Sensitivity analysis was performed to see the different features between the conventional method and the proposed method. For exchange coefficients, one parameter was manipulated, and the others were fixed as the values estimated by each MFA method. Each manipulated exchange coefficient was varied within a range from 0 to 0.95. The CE–TOFMS-measured intermediates analyzed included glucose-6-phosphate (G6P), fructose-6-phosphate (F6P), fructose-1,6-bisphosphate (F16P), dihydroxyacetone phosphate (DHAP), 3-phosphoglycerate (3PG), phosphoenolpyruvate (PEP), pyruvate (PYR), ribulose-5-phosphate (Ru5P), ribose-5-phosphate (R5P), sedoheptulose-7-phosphate (S7P), 2-oxoglutarate (αKG), and malate (MAL); the GC–MS-measured amino acids included Ala, Asp, Met, Glu, Pro, Ser, Gly, Val, Ile, Phe and Tyr.

3. Results and discussion

3.1. Measurement of mass distributions of intracellular metabolites by CE–TOFMS

Table 1 is a summary of the mass distributions of the intracellular metabolites in cells cultured at dilution rates of 0.1 and 0.5 h^{-1}. The intermediate metabolites of the central carbon metabolism are precursors of the amino acids. Therefore, we compared the mass distributions of the precursor metabolites for amino acid biosynthesis measured by CE–TOFMS with those of the fragment ion ($[M-57]^+$) of the corresponding TBDMS-amino acid measured by GC–MS (Fig. 1). In the pathways we investigated, the intact carbon skeleton of 3PG,

Table 1
Mass distributions of the intracellular metabolites in *E. coli* measured by CE–TOFMS

Dilution rate (h^{-1})	Metabolite	Mass distribution							
		m_0	m_1	m_2	m_3	m_4	m_5	m_6	m_7
0.1	G6P	0.419	0.216	0.114	0.114	0.036	0.047	0.055	
	F6P	0.332	0.194	0.139	0.156	0.068	0.045	0.067	
	F16P	0.391	0.228	0.118	0.138	0.047	0.022	0.056	
	DHAP	0.599	0.176	0.080	0.145				
	3PG	0.643	0.155	0.068	0.135				
	PEP	0.552	0.261	0.000	0.187				
	PYR	0.627	0.210	0.041	0.123				
	S7P	0.310	0.240	0.153	0.150	0.082	0.039	0.017	0.009
	Ru5P	0.444	0.232	0.154	0.108	0.029	0.033		
	R5P	0.433	0.221	0.165	0.124	0.032	0.026		
	E4P	0.582	0.158	0.000	0.260	0.000			
	AKG	0.402	0.259	0.204	0.088	0.038	0.010		
	MAL	0.442	0.264	0.207	0.064	0.023			
0.5	G6P	0.473	0.206	0.040	0.124	0.035	0.063	0.059	
	F6P	0.371	0.159	0.186	0.091	0.032	0.059	0.101	
	F16P	0.385	0.222	0.127	0.131	0.082	0.053	0.000	
	DHAP	0.632	0.208	0.000	0.161				
	3PG	0.636	0.148	0.069	0.147				
	PEP	0.612	0.164	0.083	0.141				
	S7P	0.388	0.207	0.127	0.123	0.086	0.046	0.024	0.000
	Ru5P	0.476	0.233	0.171	0.120	0.000	0.000		
	R5P	0.455	0.199	0.224	0.122	0.000	0.000		
	E4P	0.518	0.158	0.132	0.192	0.000			
	MAL	0.435	0.254	0.194	0.088	0.030			

m_n represents the isotopomer abundance for each metabolite in which n ^{13}C atoms are incorporated.

PYR, and αKG is maintained in the corresponding products, Ser, Ala, and Glu, respectively. These intermediate metabolites and proteinogenic amino acids were used for comparisons. As shown in Fig. 1, the mass distribution of fragment ions of Glu was similar to that of αKG. However, the m_0 values of Ser and Ala were higher than those of the corresponding metabolites, 3PG and PYR. In this study, the mass distributions of proteinogenic amino acid were corrected to achieve isotopic steady state [20] as described in Section 2.6. These corrections were carried out based on the standard wash-out kinetics of a continuous stirred tank reactor (CSTR). However, this correction neglects protein turnover between proteinogenic amino acid and free amino acid pools, and transamination reactions where amino acids such as glutamate and aspartate exchange amino group via central metabolites such as αKG and OAA. Grotkjaer et al. [21] demonstrated by simulation studies that protein turnover and transamination may cause large deviation of labeling kinetics from that of the simple CSTR. Furthermore, Wiechert and Nöh [8] indicated the ratios between intermediate metabolite pool size and corresponding proteinogenic amino acid pool size, not incorporated in our correction for isotopic steady state, to have critical impact on the labeling kinetics. In addition, they also pointed out that the topology of the pathway (e.g. cyclic or liner) has influence on the labeling kinetics [8]. The differences of mass distributions between proteinogenic amino acid and corresponding precursor metabolites in Fig. 1 were considered to be derived from combinations of these factors. These results suggest that the generally used correction method for isotopic steady state based on CSTR kinetics for proteinogenic amino acids is not always enough to estimate the true labeling pattern at an isotopic steady state.

3.2. A new MFA based on the mass distributions of intracellular metabolites measured by CE–TOFMS

A summary of the chemostat cultures is shown in Table 2. The ^{13}C-labeled intermediate metabolites and proteinogenic amino acids were obtained from the same culture samples, and the mass distributions were analyzed by CE–TOFMS and GC–MS, respectively. Fig. 2 shows the flux distributions at each dilution rate estimated by the new and the conventional method. To validate the accuracy of the each flux estimation, the mass distributions of intermediate metabolites simulated from the metabolic flux distributions were compared with the measured mass distributions (Fig. 3). We could confirm that there was high correlation between measured and simulated mass distributions

Table 2
Summary of glucose-limited chemostat cultures of *E. coli* at various specific growth rates

Specific rate (mmol g of dry cell^{-1} h^{-1})	Specific growth rate	
	0.1 h^{-1}	0.5 h^{-1}
Glucose uptake	1.34	6.62
Acetate production	0.00	0.49
Ethanol production	0.00	0.15
O_2 uptake	2.20	13.05
CO_2 evolution	0.31	8.95

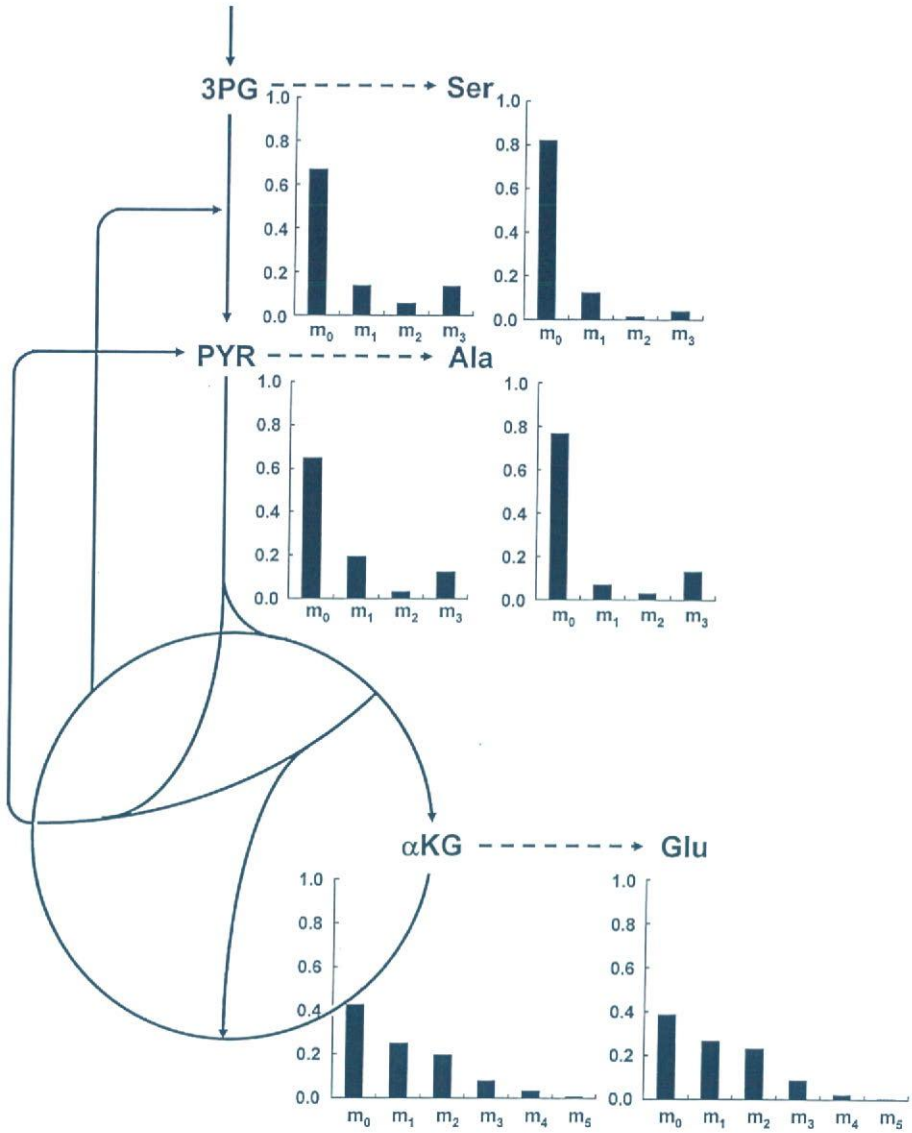

Fig. 1. Comparison between mass distributions of precursor metabolites and proteinogenic amino acids at the dilution rate of 0.1 h^{-1}. The mass distributions were corrected by taking into account natural isotope abundance.

at each dilution rate. In the new MFA method, the correlation coefficients were 0.98 and 0.97 for the dilution rates of 0.1 and 0.5 h^{-1}, respectively. On the other hand, in the conventional MFA method, the correlation coefficients were 0.99 and 0.98 for the dilution rates of 0.1 and 0.5 h^{-1}, respectively. These results indicate the flux calculations by both methods can be performed successfully. The fluxes of glycolysis estimated by the new method were lower than those obtained by the conventional method, while the overall net flux distributions obtained by the two MFA methods showed good agreement. The difference in glycolytic fluxes was derived from the differences in mass distributions between precursor metabolite and corresponding amino acid in glycolysis, as described above.

Our new approach facilitates high-throughput flux analysis without requiring complicated sample preparations such as hydrolysis of proteins and derivatization of amino acids, as mentioned in Section 1. Thus, the sample preparation time was shortened from 2–3 days to 6 h.

3.3. Sensitivity analysis of the mass distributions for exchange coefficient

As shown in Fig. 2, the exchange fluxes for reversible reactions, except for v_2, were different in the two MFA methods. Thus, we made sensitivity analysis of the exchange coefficients to clarify the reason underlying the difference in the exchange coefficients. Each exchange coefficient was varied within a predetermined range from 0 to 0.95, and following changes in the mass distributions of intracellular metabolites and amino acids were simulated. In the MFA procedure, unknown variables, including the exchange coefficient, are assumed, and mass distributions of metabolites and fluxes of extracellular metabolites

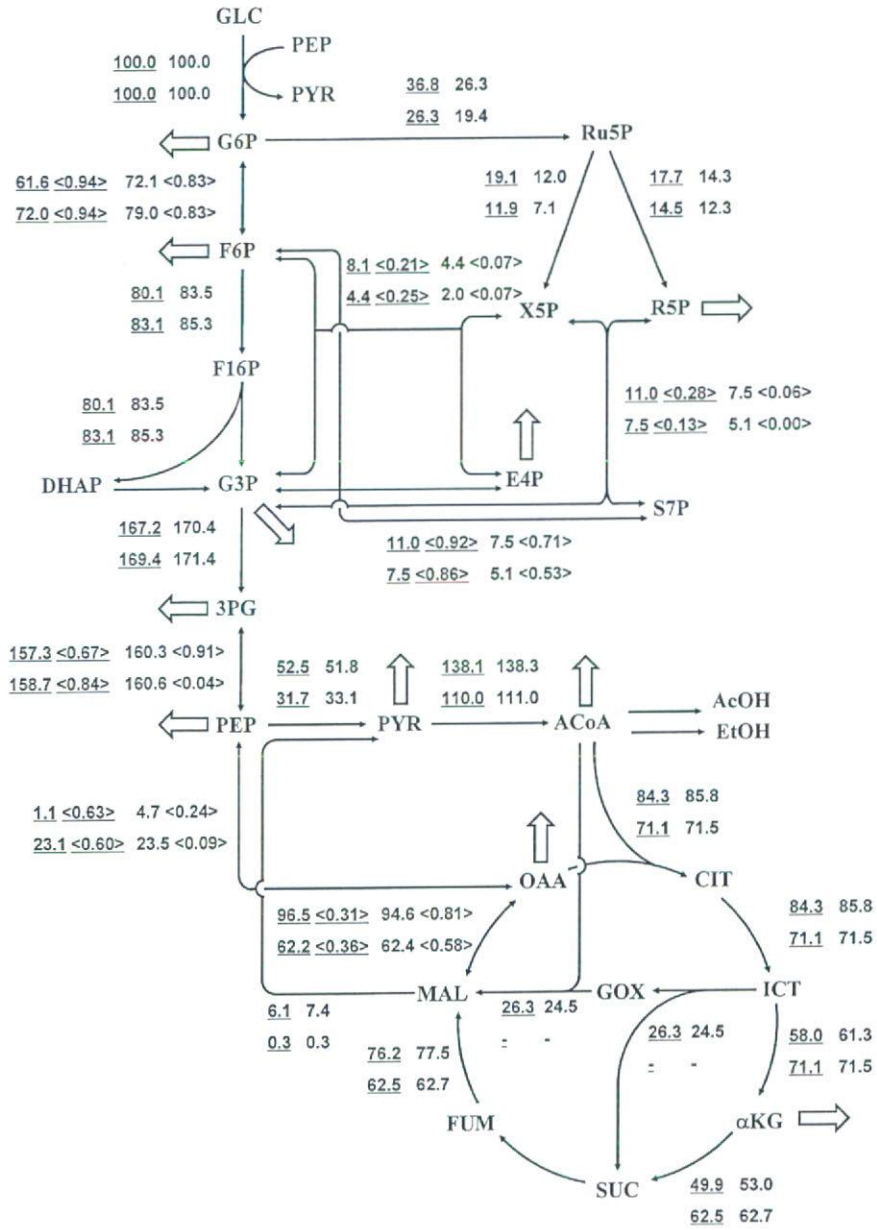

Fig. 2. Metabolic flux distributions of the central carbon metabolism in *E. coli* estimated by the new (underlined) and the conventional MFA at specific growth rates of 0.1 (upper value) and 0.5 (lower value) h^{-1}. All fluxes are given as relative values to the specific glucose consumption rate and are expressed as net fluxes. Fluxes for biomass synthesis are indicated by open arrows. GLC, glucose; G3P, glyceraldehyde-3-phosphate; X5P, xylulose-5-phosphate; E4P, erythrose-4-phosphate; ACoA, acetyl-CoA; OAA, oxaloacetate; CIT, citrate; ICT, isocitrate; SUC, succinate; FUM, fumarate; GOX, glyoxylate; AcOH, acetate; EtOH, ethanol.

and biomass synthesis are simulated using the assumed variables. The simulated and measured mass distributions and fluxes of extracellular metabolites and biomass synthesis are then compared and the differences are incorporated as the fitness function J. Thus, if the mass distributions are highly sensitive to a change in the exchange coefficient, the range of fitness function becomes large, and selection of the superior solution becomes easy. The number of such sensitive metabolites is also related to the ease of flux estimation.

As shown in Fig. 4A, changes in $exch_{13}$ affected the mass distributions of metabolites and amino acids related to the glycolysis and the pentose phosphate pathway. The features of $exch_{14}$ and $exch_{15}$ were similar to those of $exch_{13}$. In the compounds that were sensitive to changes in the exchange coefficient, the number of CE–TOFMS-measured metabolites was larger than the number of GC–MS-measured proteinogenic amino acids. Additionally, the changes in the mass distributions of the intermediate metabolites were larger than those of the proteinogenic amino acids. These results indicate that $exch_{13}$, $exch_{14}$, and $exch_{15}$ can be estimated more easily by the new MFA method than the conventional one. Furthermore, in the new MFA method, these exchange coefficients were determined

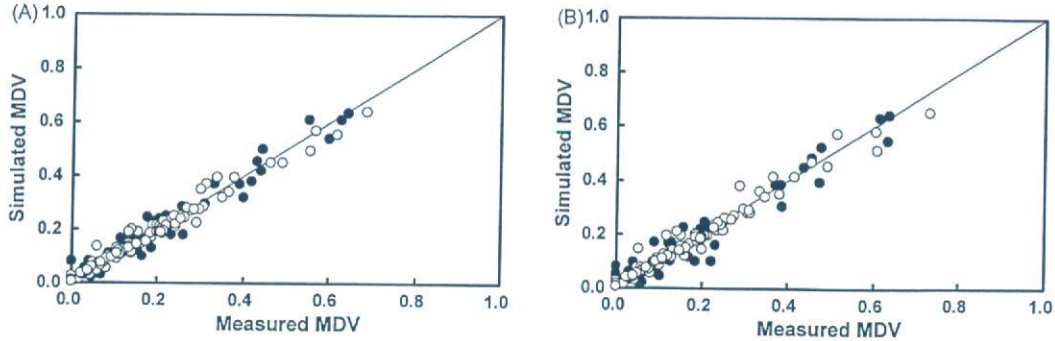

Fig. 3. Comparison of mass distributions of metabolites simulated from the estimated fluxes with those measured by CE–TOFMS or GC–MS. Comparisons at the dilution rate of 0.1 h^{-1} (A) and 0.5 h^{-1} (B) are shown. Closed circles, intermediate metabolites; open circles, proteinogenic amino acids.

by mass distributions of G6P, F6P, F16P, DHAP, 3PG, PEP, PYR, Ru5P, R5P and S7P. On the other hand, in the conventional MFA method, these exchange coefficients were determined by mass distributions of Gly and Ser, both of which are derived from 3PG. Thus, the differences in the exchange coefficient values estimated by the two methods are ascribable to the differences in labeling information obtained by two MFA.

On the other hand, as shown in Fig. 4B, changes in $exch_{23}$ affected the mass distributions of intermediate metabolites and amino acids related to the lower part of glycolysis and the TCA cycle including 3PG, PEP, PYR, αKG, MAL, Ala, Asp, Glu, Pro, Ser, Gly, Val, Phe, Tyr. We found that the mass distributions of the precursor metabolites (3PG and PYR) were different from those of the proteinogenic amino acids (Ser and Ala). Consequently, the exchange coefficients estimated by the new and the conventional MFA methods were different. Although such differences in the exchange coefficient were observed, the estimated net flux of v_{23} matched well between the new and the conventional MFA method.

The simulation result revealed that $exch_7$ had almost no effect to the change in mass distributions of most metabolites measured by CE–TOFMS and GC–MS (Fig. 4C). This result is consistent with the report by Zhao and Shimizu [16]; the exchange coefficient for enolase ($exch_7$ in the present study) was not reliable because the region of confidence was extremely large. Furthermore, the feature of simulation result of $exch_{22}$ was similar to that in $exch_7$ (data not shown). Therefore, the $exch_7$ and $exch_{22}$ were not estimated in this study.

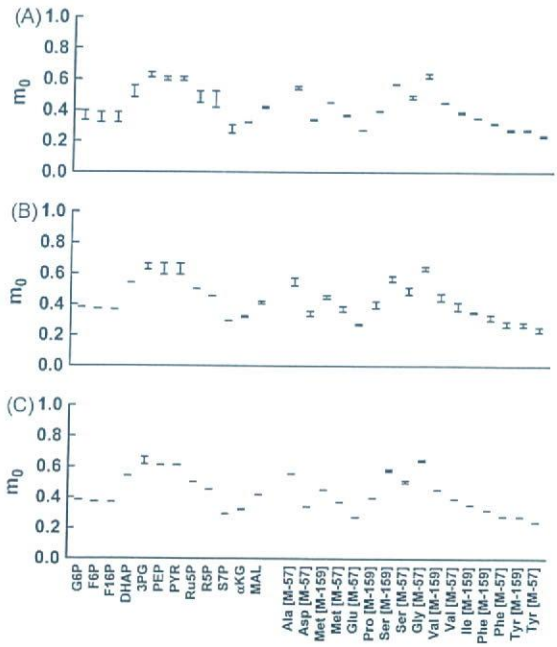

Fig. 4. Effect of changes in exchange coefficients on the mass distributions of metabolites. The effect of a change in the exchange coefficient for reversible flux on the mass distributions of metabolites was simulated using the flux at 0.1 h^{-1} calculated by the new MFA method. The simulation results for $exch_{13}$ (A), $exch_{23}$ (B) and $exch_7$ (C) are shown. In this figure, the change in m_0 is shown.

4. Conclusions

We applied our new CE–TOFMS method for measuring mass distributions of intracellular metabolites in MFA. The proposed MFA method yields advantages over the conventional method. In particular, the new approach facilitates high-throughput flux analysis without requiring complicated sample preparations such as hydrolysis of proteins and derivatization of amino acids. Thus, the sample preparation time was shortened from 2–3 days to 6 h.

Additionally, because the new MFA method is based on isotope labeling patterns of intracellular free metabolites, it can be applied to cultivation using amino acid(s) as a carbon source(s). Furthermore, since the pool size of the intermediate metabolites is generally very small, there is an immediate turnover of metabolites; and in intermediate metabolites, changes in the labeling patterns of upstream metabolites are reflected quickly. Thus, a change in metabolism at the instant of an environmental change can be captured by observation of the intermediate metabolites. Therefore, the new approach proposed here can be applied to batch or fed-batch cultures. Studies are underway in our laboratory to examine the applicability of our new method under conditions where the metabolism of the cultured cells varies with the term of the culture.

Acknowledgments

We thank Pei Yee Ho for insightful discussions. This study was carried out as part of The Project for Development of a Tech-

nological Infrastructure for Industrial Bioprocesses on R&D of New Industrial Science and Technology Frontiers of the Ministry of Economy, Trade & Industry (METI), under the auspices of the New Energy and Industrial Technology Development Organization (NEDO). This work was also made possible by research funds from the Yamagata Prefectural Government and Tsuruoka City.

Appendix A. Metabolic reaction model for MFA

Flux	Reaction
v_1	GLC + PEP → G6P + PYR
v_2	G6P ↔ F6P
v_3	F6P → F16P
v_4	F16P → G3P + DHAP
v_5	DHAP → G3P
v_6	G3P → 3PG
v_7	3PG → PEP
v_8	PEP ↔ PYR
v_9	PYR → ACoA + CO_2
v_{10}	G6P → Ru5P + CO_2
v_{11}	Ru5P → R5P
v_{12}	Ru5P → X5P
v_{13}	R5P + X5P ↔ S7P + G3P
v_{14}	S7P + G3P ↔ F6P + E4P
v_{15}	X5P + E4P ↔ F6P + G3P
v_{16}	ACoA + OAA → CIT
v_{17}	CIT → ICT
v_{18}	ICT → αKG + CO_2
v_{19}	αKG → SUC + CO_2
v_{20}	SUC → FUM
v_{21}	FUM → MAL
v_{22}	MAL ↔ OAA
v_{23}	PEP + CO_2 ↔ OAA
v_{24}	MAL → PYR + CO_2
v_{25}	ICT → GOX + SUC
v_{26}	GOX + ACoA → MAL

References

[1] A. Roscher, N.J. Kruger, R.G. Ratcliffe, J. Biotechnol. 77 (2000) 81.
[2] B.D. Follstad, R.R. Balcarcel, G. Stephanopoulos, D.I. Wang, Biotechnol. Bioeng. 63 (1999) 675.
[3] E. Fischer, N. Zamboni, U. Sauer, Anal. Biochem. 325 (2004) 308.
[4] T.L. Nissen, U. Schulze, J. Nielsen, J. Villadsen, Microbiology 143 (1997) 203.
[5] B. Christensen, J. Nielsen, Metab. Eng. 1 (1999) 282.
[6] W. Wiechert, Metab. Eng. 3 (2001) 195.
[7] K. Shimizu, Adv. Biochem. Eng. Biotechnol. 91 (2004) 1.
[8] W. Wiechert, K. Nöh, Adv. Biochem. Eng. Biotechnol. 92 (2005) 145.
[9] W.A. van Winden, J.C. van Dam, C. Ras, R.J. Kleijn, J.L. Vinke, W.M. van Gulik, J.J. Heijnen, FEMS Yeast Res. 5 (2005) 559.
[10] T. Soga, R. Baran, M. Suematsu, Y. Ueno, S. Ikeda, T. Sakurakawa, Y. Kakazu, T. Ishikawa, M. Robert, T. Nishioka, M. Tomita, J. Biol. Chem. 281 (2006) 16768.
[11] R. Baran, H. Kochi, N. Saito, M. Suematsu, T. Soga, T. Nishioka, M. Robert, M. Tomita, BMC Bioinform. 7 (2006) 530.
[12] A. Buchholz, J. Hurlebaus, C. Wandrey, R. Takors, Biomol. Eng. 19 (2002) 5.
[13] T. Soga, Y. Ohashi, Y. Ueno, H. Naraoka, M. Tomita, T. Nishioka, J. Proteome Res. 2 (2003) 488.
[14] K.A. Siddiquee, M.J. Arauzo-Bravo, K. Shimizu, FEMS Microbiol. Lett. 235 (2004) 25.
[15] W. Wiechert, C. Siefke, A.A. de Graaf, A. Marx, Biotechnol. Bioeng. 55 (1997) 118.
[16] J. Zhao, K. Shimizu, J. Biotechnol. 101 (2003) 101.
[17] M. Li, P.Y. Ho, S. Yao, K. Shimizu, J. Biotechnol. 122 (2006) 254.
[18] A. Nanchen, A. Schicker, U. Sauer, Appl. Environ. Microbiol. 72 (2006) 1162.
[19] W.A. van Winden, C. Wittmann, E. Heinzle, J.J. Heijnen, Biotechnol. Bioeng. 80 (2002) 477.
[20] M. Dauner, J.E. Bailey, U. Sauer, Biotechnol. Bioeng. 76 (2001) 114.
[21] T. Grotkjaer, M. Akesson, B. Christensen, A.K. Gombert, J. Nielsen, Biotechnol. Bioeng. 86 (2004) 209.

EXPERIMENTAL MEDICINE
実験医学 月刊

別　刷

羊土社
〒101-0052
東京都千代田区神田小川町2-5-1 神田三和ビル
TEL：03-5282-1211（代表）　FAX：03-5282-1212
E-mail：eigyo@yodosha.co.jp
URL：http://www.yodosha.co.jp/

実験医学

Vol.26-No. 1　2008

[特集]

メタボローム

—代謝研究の新潮流

代謝プロファイル,低酸素応答,タンパク質機能解析と肥満・炎症メカニズムの解明から食品開発まで

企画／曽我朋義

オミクス（-omics）研究の目的は，予想不可能な生体内の環境変化をバイアスをかけない手法により包括的に探索することである．近年の分析技術，データ処理技術の発展により代謝産物の総称であるメタボロームの解析環境も整いつつあり，メタボローム研究から興味深い生命現象の知見が得られ，産業応用にまで発展してきた．本特集では，各分野で活躍中の第一線の研究者に最近の研究成果を紹介していただいた．　（曽我朋義）

概論

メタボロームが解き明かす生命のシステム

―技術革新がもたらす生命科学の新時代

曽我朋義

はじめに

トランスクリプトミクス，プロテオミクス，メタボロミクス等のオミクス研究は，細胞や生体内の多数の構成成分の変化をバイアスをかけない手法により網羅的に探索し，生命現象を包括的に理解しようとするものである．従来の仮説検証型の科学に対して，オミクス研究は網羅的なデータ解析によって背後に隠れている因子を見つけ出そうとする仮説発見型研究であり，人が予想もしていなかった大発見をもたらす可能性を秘める．

近年のポストゲノム研究の進展に伴い，細胞内化合物の網羅的・包括的な測定法が急速に発達した．トランスクリプトームに関してはDNAマイクロアレイの登場によって遺伝子発現の大規模測定が実現した．プロテオームに関しても，膜タンパク質など測定が難しいものが存在するものの，高速液体クロマトグラフィー―質量分析計（LC-MS）や二次元電気泳動法の開発によって網羅的な測定が可能になった．トランスクリプトームの測定対象であるmRNAはおもに4種類の核酸，またプロテオームの測定対象であるタンパク質は，リン酸や糖鎖の修飾はあるものの基本的に20種類のアミノ酸から構成されているため，標準物質がなくても最新の測定技術とデータベースを用いれば比較的簡単に同定することが可能である．しかし，トランスクリプトミクス，プロテオミクスでは，分子間の相互作用やネットワークに関する情報の蓄積やデータベースはほとんどなく，それらの解析は今後の課題となっている．

全代謝物質の網羅的な解析を目指すメタボロミクスでは，多様な代謝物質が存在し，代謝標準物質も20％程度しか入手できない状況においては，未知物質の特定がきわめて難しく，それがこの研究分野の進展の障壁となっている．一方，代謝経路の解明は進んでおり，KEGG（http://kegg.jp/），MetaCyc（http://metacyc.org/）等，いくつかのデータベースがすでに構築されているため，代謝物質間や代謝物と酵素の関係，ネットワークはかなり明らかになっている．

代謝産物には物理的化学的性質が非常に似かよったものから全く異なるものまで多くの化合物が混在し，それらを区別してかつ同時に測定することがきわめて難しかった．一方メタボローム研究への関心の高まりに伴い，ガスクロマトグラフィー―質量分析計（GC-MS）[1]，

Metabolomics - a new approach to elucidating biosystems

Tomoyoshi Soga：Institute for Advanced Biosciences, Keio University（慶應義塾大学先端生命科学研究所）

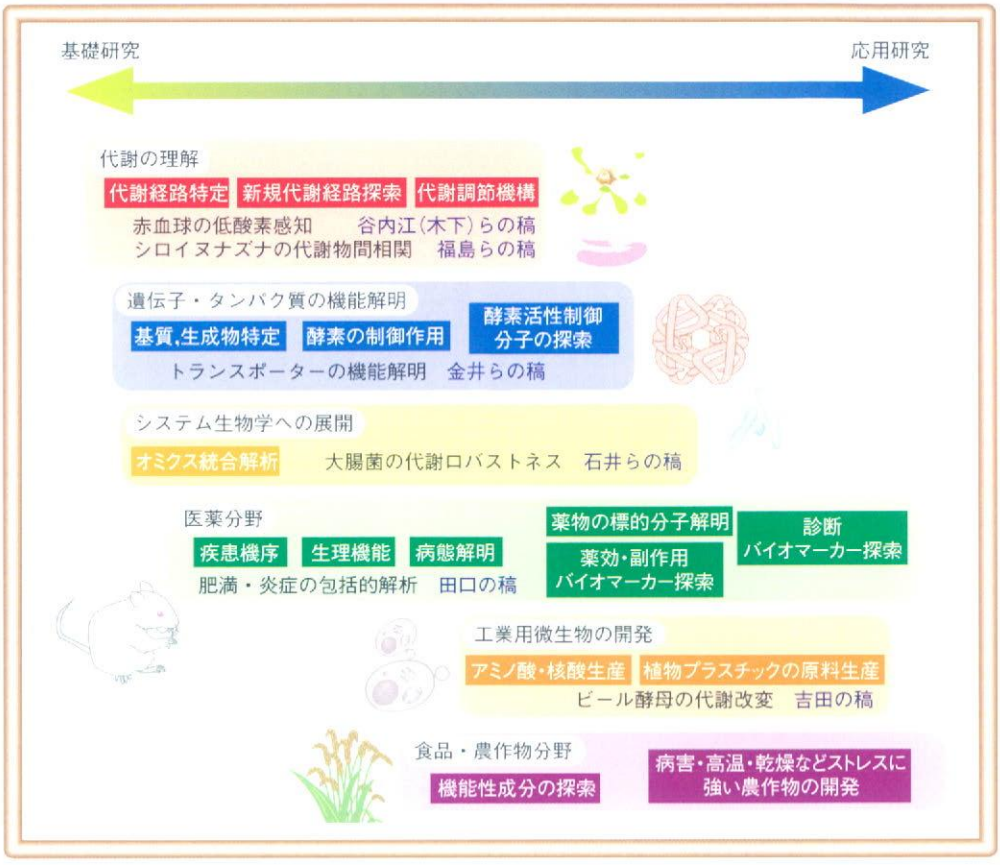

概念図　各種メタボローム研究の位置付け
近年，メタボローム解析は，代謝の解明，遺伝子やタンパク質の機能解析等の基礎研究から医薬，発酵，食品，農作物分野の応用研究まで幅広く行われている

LC-MS[2]，キャピラリー電気泳動－質量分析計（CE-MS）[3][4]，フーリエ変換イオンサイクロトロン共鳴質量分析（FT-ICRMS）[5]，核磁気共鳴装置（NMR）[6]など（それぞれに測定対象，感度，定量性，網羅性，スループットに長所と短所があるが），いくつかのメタボローム測定法が開発された．近年これらの方法論によって急速に発展したメタボローム研究が，ゲノム，トランスクリプトーム，プロテオーム情報と組合わさった結果，代謝調節機構の解明[7][8]，遺伝子やタンパク質の機能解明[9][10]などの基礎研究から，医薬品の副作用のメカニズムや早期検出可能なバイオマーカー探索[1]，食品に含まれる機能性成分の探索，工業用微生物の育種などの産業応用に有用であることが示されてきた．本特集では，興味深い最新のメタボロミクスの研究成果を第一線の研究者の方に紹介していただいた．

1 赤血球の酸素応答機構の解明〔谷内江（木下）らの稿〕

谷内江（木下）らは，メタボローム測定とコンピュータシミュレーションによって赤血球の代謝調節機構を解明した．代謝赤血球内の代謝反応ネットワークとヘモグロビンの酸素運搬